 doi:10.20944/preprints202203.0410.v1



*Article*

# Cross-sectional Analysis of Beams Subjected to Saint-Venant Torsion Using the Green's Theorem and the Finite Difference Method

**Valentin Fogang**

Civil Engineer, C/o BUNS Sarl, P.O Box 1130, Yaounde, Cameroon; valentin.fogang@bunscameroun.com

valentinfogang@yahoo.de ORCID iD https://orcid.org/0000-0003-1256-9862

**Abstract:** This paper presents an approach to the elastic analysis of beams subjected to Saint-Venant torsion using Green's theorem and the finite difference method (FDM). The Saint-Venant torsion of beams, also called free torsion or unrestrained torsion, is characterized by the absence of axial stresses due to torsion; only shear stresses are developed. The solution to this torsion problem consists of finding a stress function that satisfies the governing equation and the boundary conditions. The FDM is an approximate method for solving problems described with differential or partial differential equations; it does not involve solving differential equations, equations are formulated with values at selected nodes of the structure. In this paper, the beam's cross-section was discretized with a two-dimensional grid and additional nodes were introduced at the boundaries. The introduction of additional nodes allowed us to apply the governing equations at boundary nodes and satisfy the boundary conditions. Beam's cross-sections of various shapes and openings were analyzed using this model; shear stresses, torsion constant, and warping were determined. Furthermore, beams with thin-walled closed sections, single-cell or multiple-cell, were analyzed using the stress function whereby the linear distribution of the shear stresses over the thickness was considered; closed-form solutions for shear stresses and torsion constant were presented. For rectangular cross-sections, the results obtained in this study showed good agreement with the exact results, and the accuracy was increased through a grid refinement. For thin-walled closed sections the values of torsion constant and maximal shear stress were higher than those calculated using Bredt's analysis; moreover, regarding the closed-form solution, the maximal shear stress in the cross-section does not necessarily occur at the position with the smallest thickness.

**Keywords:** Theory of elasticity; Saint-Venant torsion; Green's theorem; finite difference method; additional nodes; thin-walled sections; cross-section with openings; warping

## 1. Introduction

This paper describes the application of Fogang's model [1] based on the finite difference method (FDM), used for the homogeneous Euler–Bernoulli beam, to the elastic analysis of beams subjected to Saint-Venant torsion. The Saint-Venant torsion is characterized by the absence of axial stresses due to torsion; only shear stresses are developed. The correct solution of the problem of torsion of prismatical beams was given by Saint-Venant [2]; he made assumptions on the deformation of the twisted bar that could satisfy the equations of equilibrium and the boundary conditions.

Preprints (www.preprints.org) | NOT PEER-REVIEWED | Posted: 31 March 2022 doi:10.20944/preprints202203.0410.v1



Prandtl [3] introduced a stress function in terms of which the shear stresses were defined. Therefore, the solution of the torsion problem consists of finding a stress function which satisfies the governing equation and the boundary conditions. Analytical solutions of the stress function are available for beams with elliptical cross-sections and equilateral triangle; furthermore, the torsional problem was solved for rectangular cross-section using infinite trigonometric series. However, analytical solutions of the Saint-Venant torsion are only suitable for simple cross-sections; therefore, numerical methods to evaluate the torsional behavior of complicated cross-sections are indispensable. Numerical methods such as energy methods were considered by numerous authors i.e. Ritz [4] and Trefftz [5]; the stress function was approximately determined from the minimum condition of the strain energy of the twisted beam. Furthermore, various studies have focused on the analysis of beams under unrestrained torsion. Pluzsik et al. [6] presented a theory for thin-walled, closed section, orthotropic beams which takes into account the shear deformation in restrained warping induced torque; the analytical ("exact") solution of simply supported beams subjected to a sinusoidal load was developed for this purpose. Pan et al. [7] presented a matrix stiffness method for the torsion and warping analysis of beam-columns in order to investigate the exact element torsional stiffness considering warping deformations; the equilibrium analysis of an axial-loaded torsion member was conducted, and the torsion-warping problem was solved based on a general solution of the established governing differential equation for the angle of twist. Pavazza et al. [8] presented a novel theory of torsion of thin walled beams ("shear deformable beams") of arbitrary open cross-sections with influence of shear; the theory is based on the classical Vlasov's theory of thin-walled beams of open cross-section, as well on the Timoshenko's beam bending theory. Choi & Kim [9] proposed a higher-order Vlasov torsion theory that not only includes as many torsion-related modes as desired but also provides the explicit forces–kinematic variables–stresses relationships that are fully consistent with those by the Vlasov theory. Amulu & Ezeagu [10] investigated the effect of combined actions of torsion moments, bending moments and shear forces in reinforced concrete beams with concrete compressive strength of $30N/mm^2$; the ultimate torsion moments, bending moments, and shear forces of the beams were determined experimentally. Tran [11] used isoparametric eight-noded quadrilateral elements in order to improve Gruttmann's isoparametric four-noded quadrilateral elements; MATLAB was the language for programming the numerical method.

In this paper the torsion problem of beams with solid cross-sections was solved using FDM. The cross-sections were discretized with a two-dimensional grid and additional nodes were introduced at the boundaries. The introduction of additional nodes allowed us to apply the governing equations at boundary nodes and to satisfy the boundary conditions. Sections with openings were also analyzed. So, the values of the stress function at nodes were determined and thereafter the shear stresses, torsion constant, and warping. Beams with thin-walled closed sections were analyzed using the stress function whereby the linear distribution of the shear stresses over the thickness was considered; closed form solutions for shear stresses and torsion constant were presented and compared to those of Bredt.

Preprints (www.preprints.org) | NOT PEER-REVIEWED | Posted: 31 March 2022 doi:10.20944/preprints202203.0410.v1



## 2. Materials and methods

### 2.1 Linear elasticity of unrestrained torsion of beams

The axis convention in the cross-section is represented in Figure 1, whereas the x-axis is the longitudinal beam's axis.

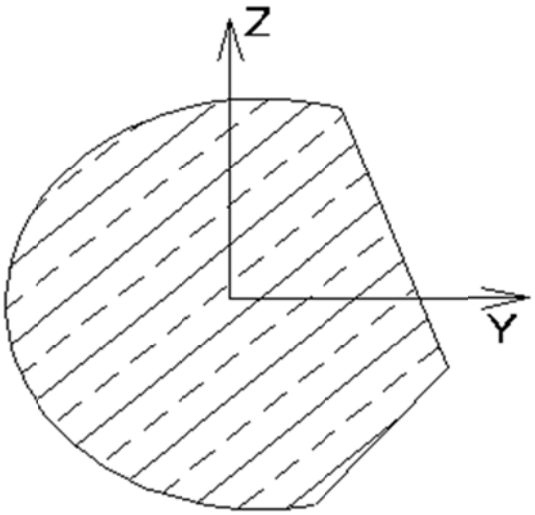


Figure 1. Axis convention within the beam's cross-section

The equations in this section are related to the theory of linear elasticity of beams. The displacements in x-, y-, and z-direction are denoted by u(x,y,z), v(x,y,z), and w(x,y,z), respectively, and the rotation of cross-section or angle of twist (positive anticlockwise) is denoted by θ(x). The shearing strains $\gamma_{xy}$ and $\gamma_{xz}$ are related to the displacements as follows:

$$\gamma_{xy} = \frac{\partial u}{\partial y} + \frac{\partial v}{\partial x}, \qquad \gamma_{xz} = \frac{\partial u}{\partial z} + \frac{\partial w}{\partial x} \tag{1a, b}$$

The cross-sections are assumed to rotate about an axis through the center of torsion $T\ (y_T, z_T)$ (which is equivalent to the shear center). Therefore, the displacements v(x,y,z) and w(x,y,z) are related to the angle of twist θ(x) as follows

$$v = -(z - z_T)\theta, \qquad w = (y - y_T)\theta \tag{2a, b}$$

Combining Equations (1a-b) and (2a-b) yields the stress strains relationships

$$\tau_{xy} = G\left(\frac{\partial u}{\partial y} - (z - z_T)\frac{d\theta}{dx}\right), \qquad \tau_{xz} = G\left(\frac{\partial u}{\partial z} + (y - y_T)\frac{d\theta}{dx}\right) \tag{3a, b}$$

where G is the shear modulus. Combining Equations (3a) and (3b) yields following relationship between the shear stresses and the rotation θ(x)

$$\frac{\partial \tau_{xy}}{\partial z} - \frac{\partial \tau_{xz}}{\partial y} = -2G\frac{d\theta}{dx} \tag{4}$$

Preprints (www.preprints.org) | NOT PEER-REVIEWED | Posted: 31 March 2022 doi:10.20944/preprints202203.0410.v1



Recalling that axial stresses do not occur in the beam subjected to unrestrained torsion, the equilibrium equation in x-direction applied to an infinitesimal beam element with dimensions dx, dy, and dz yields

$$\frac{\partial \tau_{xy}}{\partial y} + \frac{\partial \tau_{xz}}{\partial z} = 0 \tag{5}$$

Prandtl [ ] introduced a stress function $\phi(x,y,z)$, defined in terms of stress components as follows

$$\tau_{xy} = \frac{\partial \phi}{\partial z}, \qquad \tau_{xz} = -\frac{\partial \phi}{\partial y} \tag{6}$$

It is noted that Equations (6) satisfy the equilibrium equation (5). Substituting Equations (6) into (4) yields the following condition to be satisfied by the stress function $\phi(x,y,z)$

$$\frac{\partial^2 \phi}{\partial y^2} + \frac{\partial^2 \phi}{\partial z^2} = -2G\frac{d\theta}{dx} \tag{7}$$

The analysis is then reduced of determining the stress function.

Let us consider an infinitesimal beam element at the boundary with dimensions dx, dy, and dz. The tangent **t** to the boundary make an angle $\alpha$ with the +y-axis, as represented in Figure 2.

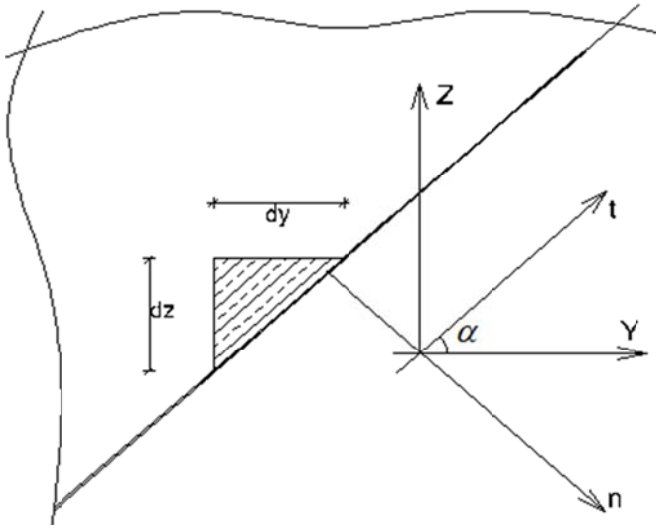


Figure 2 Infinitesimal beam element at boundary

Considering that axial stresses do not occur, the equilibrium equation applied to the beam element along the x-axis combined with Equation (6) yields

$$\begin{aligned} &\tau_{xz} dx \times dy - \tau_{xy} dx \times dz = 0 \\ &\frac{\partial \phi}{\partial y} dy + \frac{\partial \phi}{\partial z} dz = 0 \rightarrow d\phi = 0 \end{aligned} \tag{8}$$

Preprints (www.preprints.org) | NOT PEER-REVIEWED | Posted: 31 March 2022 doi:10.20944/preprints202203.0410.v1



This means that the stress function $\phi(x,y,z)$ is constant along the boundary of the cross-section. Furthermore, the shearing stress component $\tau_t$ at the boundary directed along the tangent is given by

$$\tau_t = \tau_{xy}\cos\alpha + \tau_{xz}\sin\alpha = \frac{\partial\phi}{\partial z}\cos\alpha - \frac{\partial\phi}{\partial y}\sin\alpha \tag{9a}$$

Likewise, the shearing stress component at the boundary directed along the outer normal to the boundary is given by

$$\tau_n = \tau_{xy}\sin\alpha - \tau_{xz}\cos\alpha = \frac{\partial\phi}{\partial z}\sin\alpha + \frac{\partial\phi}{\partial y}\cos\alpha = \frac{\partial\phi}{\partial y}\frac{dy}{dt} + \frac{\partial\phi}{\partial z}\frac{dz}{dt} \tag{9b}$$

Observing Equation (8), the shearing stress component $\tau_n$ is zero; this is in agreement with the condition of stress free longitudinal boundaries. Therefore, the resultant shearing stress at the boundary is $\tau_t$. Let us recall the Green's theorem which relates a line integral around a closed curve B to a double integral over the plane region A bounded by B

$$\oint_B \left[L\,dy + M\,dz\right] = \iint_A \left[\frac{\partial M}{\partial y} - \frac{\partial L}{\partial z}\right] dy\,dz \tag{10}$$

whereby L and M are functions defined on the region A and the path of integration along B is anticlockwise.

Recalling that the stress function has a constant value $\phi_B$ at the boundary, the Green's theorem shows as follows that the resultant shear forces are zero

$$\begin{aligned} \iint \tau_{xz}\,dy\,dz &= \iint -\frac{\partial\phi}{\partial y}\,dy\,dz = -\oint_B \phi\,dz = -\phi_B \oint_B dz = 0 \\ \iint \tau_{xy}\,dy\,dz &= \iint \frac{\partial\phi}{\partial z}\,dy\,dz = -\oint_B \phi\,dy = -\phi_B \oint_B dz = 0 \end{aligned} \tag{11}$$

where $\int_B$ are line integrals around the closed boundary B of the cross-section. Using Equations (6) and (11), the torque is then given by

$$M_t = \iint \left[\tau_{xz}\left(y - y_T\right) - \tau_{xy}\left(z - z_T\right)\right] dy\,dz = \iint \left[-\frac{\partial\phi}{\partial y}y - \frac{\partial\phi}{\partial z}z\right] dy\,dz \tag{12a}$$

The derivatives of $\phi y$ with respect to y and $\phi z$ with respect to z, respectively, are given by

$$\frac{\partial[\phi y]}{\partial y} = \frac{\partial\phi}{\partial y}y + \phi, \qquad \frac{\partial[\phi z]}{\partial z} = \frac{\partial\phi}{\partial z}z + \phi \tag{12b}$$

Preprints (www.preprints.org) | NOT PEER-REVIEWED | Posted: 31 March 2022 doi:10.20944/preprints202203.0410.v1



Substituting Equations (12b) into (12a) yields

$$M_t = 2\iint \phi dydz - \iint \left[ \frac{\partial [\phi y]}{\partial y} + \frac{\partial [\phi z]}{\partial z} \right] dydz \tag{12c}$$

In the case of cross-sections without openings and recalling that the stress function has a constant value $\phi_B$ at the boundary, the Green's theorem applied to the second term at the right-hand side of Equation (12c) is given by

$$\iint \left[ \frac{\partial [\phi y]}{\partial y} + \frac{\partial [\phi z]}{\partial z} \right] dydz = \oint_B [\phi y dz - \phi z dy] = \phi_B \oint_B [y dz - z dy] = 2\phi_B A_B \tag{12d}$$

where $A_B$ is the area enclosed by the outer boundary of the cross-section. Let us express the stress function as follows

$$\phi(x, y, z) = \phi_B + \phi^*(x, y, z) \tag{12e}$$

with the function $\phi^*$ being zero along the boundary and satisfying Equation (7). Substituting Equations (12d) and (12e) into (12c) yields

$$M_t = 2\iint \phi^* dydz \tag{12f}$$

Therefore, for a beam's cross-section without openings the expression of the torque is independent of the value $\phi_B$ of the stress function at the boundary. Furthermore, Equations (12a-f) show that half the torque is due to the stress component $\tau_{xy}$ and the other half to $\tau_{xz}$. For simplification purpose, a modified stress function $\psi(y,z)$ is defined as follows

$$\phi^*(x, y, z) = G \frac{d\theta}{dx} \times \psi(y, z) \tag{13a}$$

Thus, the function $\psi(y,z)$ is zero along the boundary. Substituting Equations (13a) and (12e) into (7) and (6) yields

$$\frac{\partial^2 \psi}{\partial y^2} + \frac{\partial^2 \psi}{\partial z^2} = -2 \tag{13b}$$

$$\tau_{xy} = G \frac{d\theta}{dx} \times \frac{\partial \psi}{\partial z}, \qquad \tau_{xz} = -G \frac{d\theta}{dx} \times \frac{\partial \psi}{\partial y}$$

The torsional stiffness GIt is related to the torque Mt and the angle of twist $\theta(x)$ as follows

$$M_t = GI_t \frac{d\theta}{dx} \tag{13c}$$

Preprints (www.preprints.org) | NOT PEER-REVIEWED | Posted: 31 March 2022 doi:10.20944/preprints202203.0410.v1



Combining Equations (12f), (13a), and (13c) yields the torsion constant It

$$I_t = 2\iint \psi \, dydz \tag{13d}$$

In the case of cross-sections having openings Equation (12d) becomes

$$\iint \left[ \frac{\partial[\phi y]}{\partial y} + \frac{\partial[\phi z]}{\partial z} \right] dydz = 2\phi_B A_B - \sum_i 2\phi_i A_i \tag{14a}$$

where $A_i$ are the areas enclosed by the openings i and $\phi_i$ the constant values of the stress function along the boundary of the opening i. Setting $\phi_B$ to zero and combining Equations (12c, e), (14a), and (13a, c) yield

$$I_t = 2\iint_A \psi \, dydz + 2\sum_i \psi_i A_i \tag{14b}$$

Equation (14b) can be found in Dieker [12].

## 2.2 Finite difference approximations

For simplification purpose, the analysis will be conducted in the following with the modified stress function $\psi(y,z)$. The analysis is then governed by Equation (13b-1). This equation has second order derivatives; consequently, the function $\psi(y,z)$ is approximated around the node of interest i as a second degree polynomial in each direction. The unknown at any node is the value $\psi_i$ of the modified stress function.

Given the grid spacings $\Delta y = h$ and $\Delta z = \lambda h$ in y- and z-direction, respectively. The finite difference approximations (FDAs) for the first and second derivatives are then given by

$$\left.\frac{\partial^2\psi}{\partial y^2}\right|_{i-1} = \left.\frac{\partial^2\psi}{\partial y^2}\right|_{i} = \left.\frac{\partial^2\psi}{\partial y^2}\right|_{i+1} = \frac{\psi_{i-1} - 2\psi_i + \psi_{i+1}}{h^2},$$
$$\left.\frac{\partial\psi}{\partial y}\right|_{i} = \frac{-\psi_{i-1} + \psi_{i+1}}{2h} \tag{15a, b}$$

The partial derivatives in z-direction are formulated similarly.

Preprints (www.preprints.org) | NOT PEER-REVIEWED | Posted: 31 March 2022 doi:10.20944/preprints202203.0410.v1



## 2.3 Analysis at interior nodes

### 2.3.1 Uniform grid

Figure 3 shows the node distribution of the beam's cross-section having equidistant nodes with spacings **Δy** and **Δz** in y- and z-direction, respectively. The node of interest **k** and the surrounding nodes are represented, whereby n, s, e, and w stand for the directions north, south, east, and west, respectively, according to the directions in the stencil. The node k may even be at the boundary of the beam, however being not at angles.

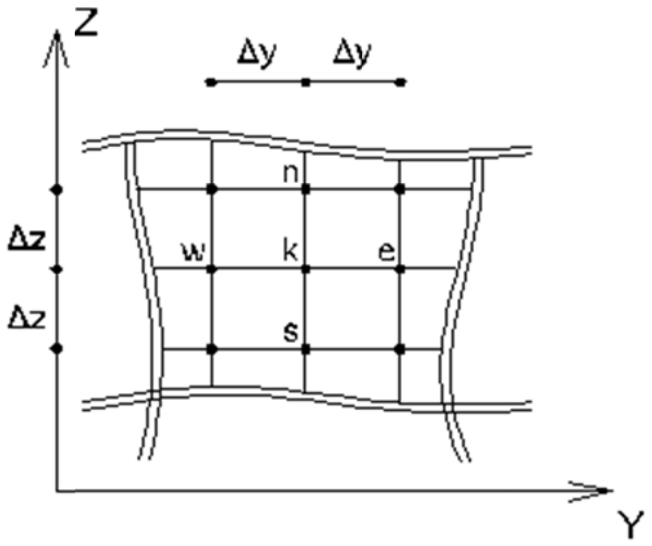


Figure 3 Node of interest **k** and its surrounding nodes for uniform grid

Given the grid spacings **Δy = h** and **Δz = λh**. The governing equation (Equation (13b-1)) at a given node can be expressed by means of a stencil using Equations (15a) as follows

$$\frac{1}{h^2}\begin{bmatrix} & \frac{1}{\lambda^2} & \\ 1 & \left[-2-\frac{2}{\lambda^2}\right] & 1 \\ & \frac{1}{\lambda^2} & \end{bmatrix}\times[\psi]=-2 \tag{16}$$

The shearing stresses are expressed using Equations (13b) and (15b) as follows

$$\tau_{xy}=G\frac{d\theta}{dx}\times\frac{1}{2\lambda h}\begin{bmatrix}1\\[0]\\-1\end{bmatrix}\times[\psi],\qquad \tau_{xz}=-G\frac{d\theta}{dx}\times\frac{1}{2h}\begin{bmatrix}-1 & [0] & 1\end{bmatrix}\times[\psi] \tag{17}$$

In the stencil notation the factor associated to the node of interest is in brackets.

Preprints (www.preprints.org) | NOT PEER-REVIEWED | Posted: 31 March 2022 doi:10.20944/preprints202203.0410.v1



### 2.3.2 Non-uniform grid

The distances to the node of interest k are represented in Figure 4 below

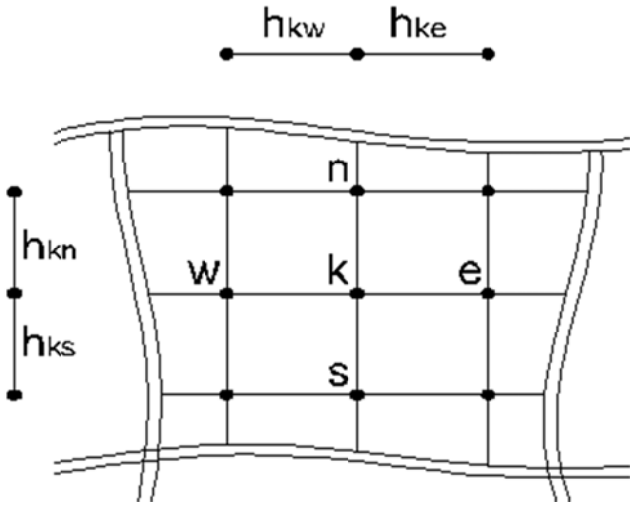


Figure 4 Node of interest **k** and its surrounding nodes for non-uniform grid

The stress function in y-direction i.e. can be described with values at grid points as follows:

$$\psi_{i-1} \times f_{i-1}(x) + \psi_i \times f_i(x) + \psi_{i+1} \times f_{i+1}(x) \tag{18a}$$

The shape functions $f_j(x)$ (j = i-1; i; i+) can be expressed using the following Lagrange interpolating polynomials

$$f_j(x) = \prod_{\substack{k=i-1 \\ k \neq j}}^{i+1} \frac{x - x_k}{x_j - x_k} \tag{18b}$$

The governing equation at node k is derived using Equations (13b-a), (18a), and (18b) as follows

$$\begin{bmatrix} & \frac{2}{h_{kn}\left(h_{kn}+h_{ks}\right)} & \\ \frac{2}{h_{kw}\left(h_{kw}+h_{ke}\right)} & \left[-\frac{2}{h_{kw}h_{ke}}-\frac{2}{h_{kn}h_{ks}}\right] & \frac{2}{h_{ke}\left(h_{kw}+h_{ke}\right)} \\ & \frac{2}{h_{ks}\left(h_{kn}+h_{ks}\right)} & \end{bmatrix} \times [\psi] = -2 \tag{19}$$

Preprints (www.preprints.org) | NOT PEER-REVIEWED | Posted: 31 March 2022 doi:10.20944/preprints202203.0410.v1



The shearing stresses are expressed using Equations (13b), (18a), and (18b) as follows

$$\tau_{xy} = G\frac{d\theta}{dx}\times\begin{bmatrix} \dfrac{h_{ks}}{h_{kn}\left(h_{kn}+h_{ks}\right)} \\ \left[\dfrac{1}{h_{ks}}-\dfrac{1}{h_{kn}}\right] \\ -\dfrac{h_{kn}}{h_{ks}\left(h_{kn}+h_{ks}\right)} \end{bmatrix}\times[\psi], \tag{20a-b}$$

$$\tau_{xz} = -G\frac{d\theta}{dx}\times\begin{bmatrix} \dfrac{-h_{ke}}{h_{kw}\left(h_{kw}+h_{ke}\right)} & \left[\dfrac{1}{h_{kw}}-\dfrac{1}{h_{ke}}\right] & \dfrac{h_{kw}}{h_{ke}\left(h_{kw}+h_{ke}\right)} \end{bmatrix}\times[\psi]$$

## 2.4 Analysis at skew edges

Figure 5 shows the skew edge of the beam's cross-section with regular and additional nodes. The tangent **t** to the skew edge makes an angle $\alpha$ with the +y-axis. One additional node is associated to each edge node; therefore, the governing equation (Equation (16) or (19)) is applied at any edge node and the boundary condition $\psi = 0$ is set.

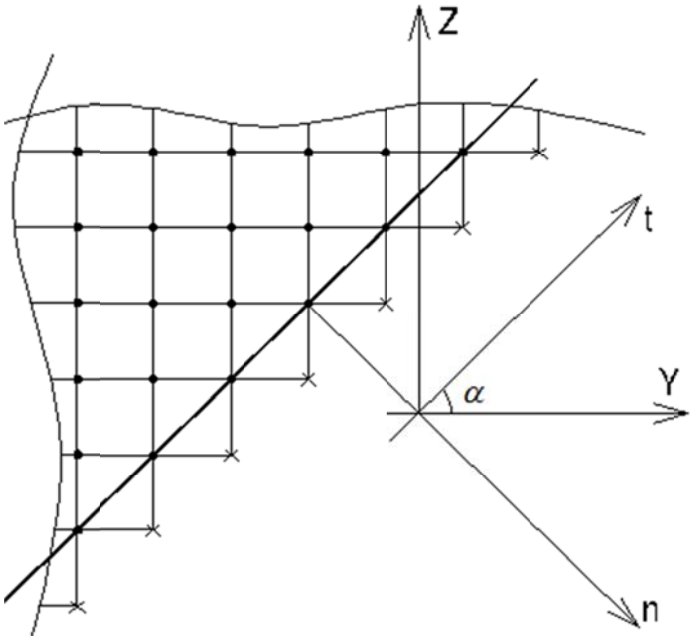


Figure 5 Skew edge of beam's cross-section with regular nodes (•) and additional nodes (×)

It is recalled that the shearing stress component $\tau_t$ directed along the tangent is calculated using Equations (9a), and the shearing stress component $\tau_{xy}$ and $\tau_{xz}$ using Equations (17) or (20a-b).

Preprints (www.preprints.org) | NOT PEER-REVIEWED | Posted: 31 March 2022 doi:10.20944/preprints202203.0410.v1



## 2.5 Analysis at beam angles

### 2.5.1 Right angles

Figure 6 below represents angles of the beam's cross-section whereby regular nodes (•) and additional nodes (×) are represented. The unknown at each node, regular or additional, is the value of the function $\psi(y, z)$. One additional node is associated to each boundary node, at which the boundary condition $\psi = 0$ is set. The governing equations at angle nodes W, E, S, and SE are modified using Equation (15a) to account for the absence of additional nodes in z-direction; Therefore Equation (21a) is the governing equation at angles W and E, while Equation (21b) is the governing equation at angles S and SE. Alternatively, additional nodes at angles could be considered in z-direction instead.

$$\frac{1}{h^2}\begin{bmatrix} 1 & \left[-2+\frac{1}{\lambda^2}\right] & 1 \\ & -\frac{2}{\lambda^2} & \\ & \frac{1}{\lambda^2} & \end{bmatrix}\times[\psi]=-2, \qquad \frac{1}{h^2}\begin{bmatrix} & \frac{1}{\lambda^2} & \\ & -\frac{2}{\lambda^2} & \\ 1 & \left[-2+\frac{1}{\lambda^2}\right] & 1 \end{bmatrix}\times[\psi]=-2 \tag{21a-b}$$

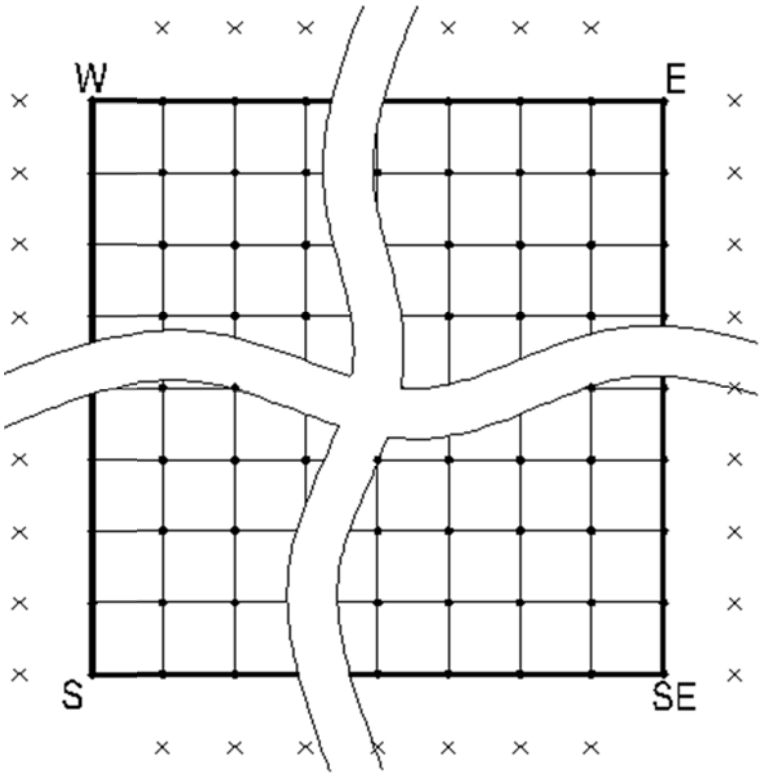


Figure 6 Angles of beam's cross-section with regular nodes (•) and additional nodes (×)

Preprints (www.preprints.org) | NOT PEER-REVIEWED | Posted: 31 March 2022 doi:10.20944/preprints202203.0410.v1



### 2.5.2 Various types of angles and shapes of beam's cross-sections

Examples of node distributions at various angles and shapes of beam's cross-sections are represented in Figure 7. The additional node associated to a node k is denoted by ka.

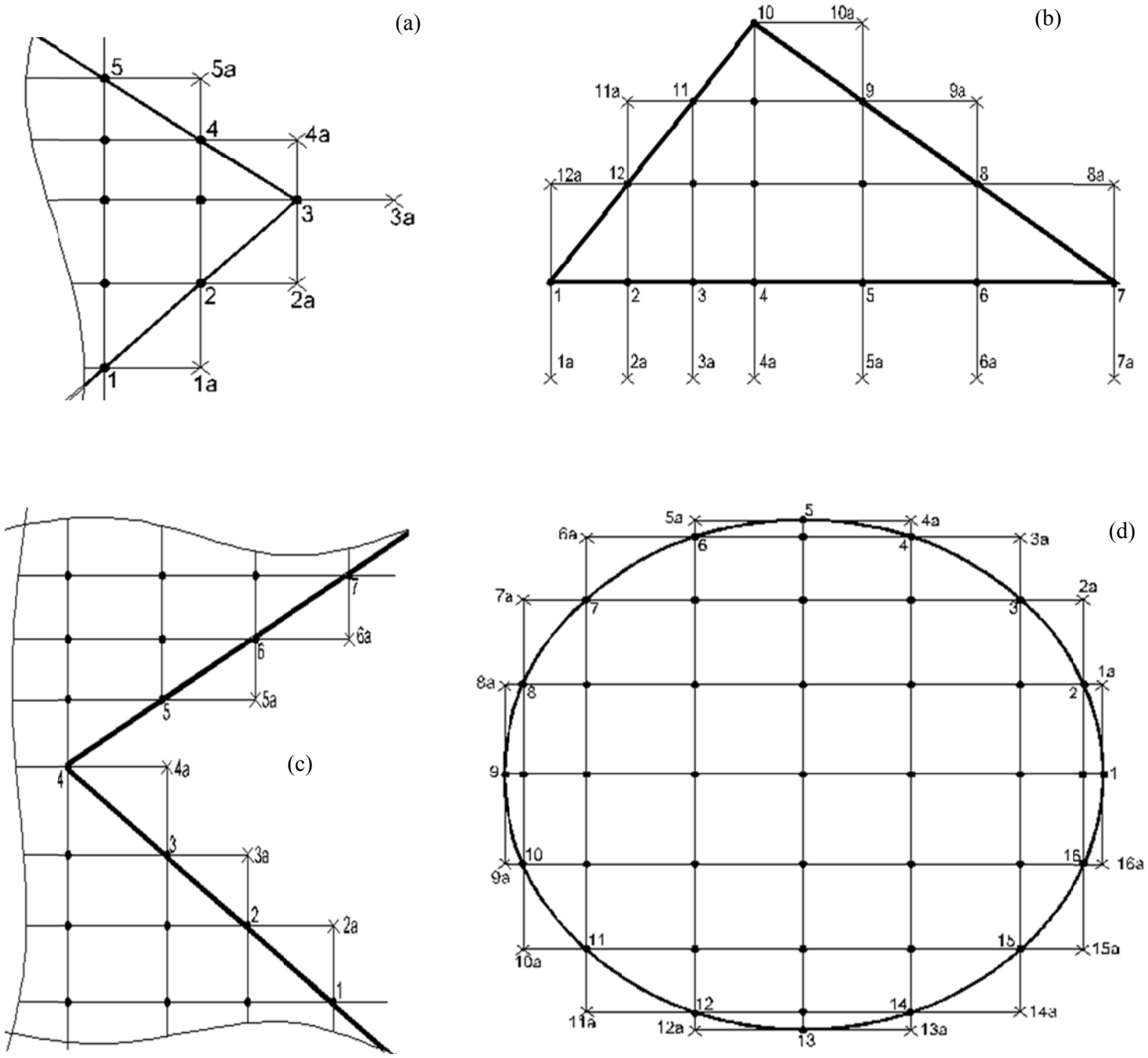


Figure 7 Examples of node distributions at various angles and shapes of beam's cross-sections

In the following the stencils may have to be modified to account for eventual non-uniform grids. Equations (16) or (19), the governing equations, are applied at any boundary node if possible. However at boundaries, priority is always given

Preprints (www.preprints.org) | NOT PEER-REVIEWED | Posted: 31 March 2022 doi:10.20944/preprints202203.0410.v1



to the satisfaction of the boundary condition $\psi = 0$. In Figure 7b, the governing equations at nodes 1 and 7, respectively, are expressed through modification of Equations (21a-b) as follows

$$\frac{1}{h^2}\begin{bmatrix} & \frac{1}{\lambda^2} & \\ \left[1-\frac{2}{\lambda^2}\right] & -2 & 1 \\ & \frac{1}{\lambda^2} & \end{bmatrix}\times[\psi]=-2, \qquad \frac{1}{h^2}\begin{bmatrix} & \frac{1}{\lambda^2} & \\ 1 & -2 & \left[1-\frac{2}{\lambda^2}\right] \\ & \frac{1}{\lambda^2} & \end{bmatrix}\times[\psi]=-2 \tag{22a-b}$$

Furthermore in Figure 7b, the distribution of additional nodes does not allow the application of the governing equation at node 10; therefore, the additional node 10a is suppressed and only the boundary condition $\psi = 0$ is applied. Consequently, at nodes 9 and 11 the governing equation is applied using Equation (21a). In Figure 7c, the governing equations at node 5 is applied using Equation (21b). In Figure 7d, the governing equations at nodes 9 and 1, respectively, are expressed using Equations (22a-b) and the governing equations at nodes 5 and 13, respectively, are expressed using Equations (21a-b).

## 2.6 Beams with openings

### 2.6.1 Openings aligned with the Cartesian coordinate system

A beam's cross-section having an opening is represented in Figure 8, together with regular nodes (•) and additional nodes (×). The opening is aligned with the Cartesian coordinate system. The unknown at regular nodes and additional nodes is the value of the stress function. The additional node associated to node k is denoted by ka.

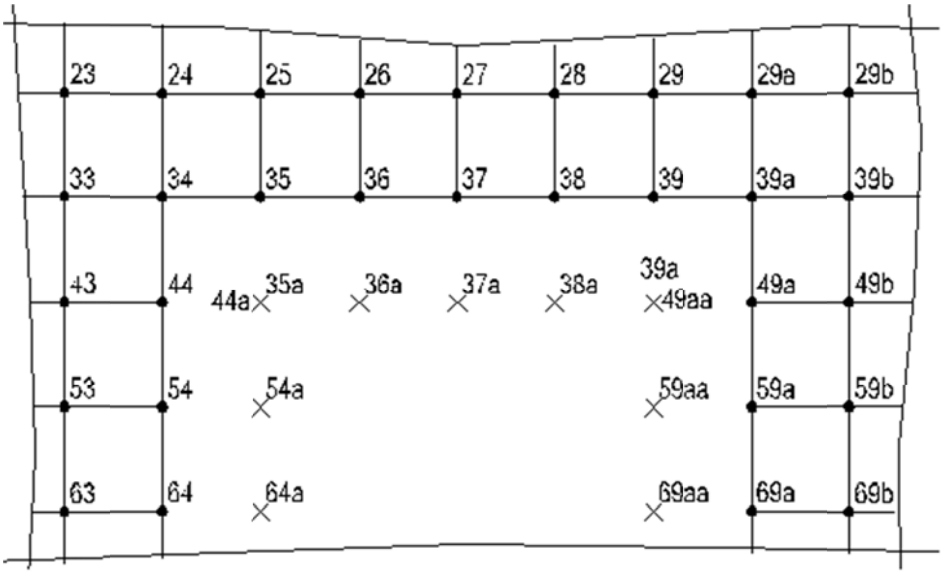


Figure 8 Beam's cross-section having an opening aligned with the Cartesian coordinate system

Preprints (www.preprints.org) | NOT PEER-REVIEWED | Posted: 31 March 2022 doi:10.20944/preprints202203.0410.v1



Similarly to Fogang […] related to the analysis of deep beams, **it is assumed that different nodes may be at the same geometrical position**, i.e. nodes 35a and 44a, 39a and 49aa in Figure 8. The boundary conditions are $\psi = 0$ at nodes on the outer boundary and $\psi$ = constant at nodes on the opening; therefore, for an opening having n nodes, n – 1 boundary conditions are applied. If additional nodes are associated to k nodes on the opening, k + 1 governing equations should be applied in order to have as many nodes as equations. Particular attention must be taken by the formulation of the governing equations and equations determining the shear stresses, especially in the vicinity of angle nodes (nodes 35, 44, 39, and 49a); those equations at any node k involve the node ka.

### 2.6.2 Openings with various shapes

A beam's cross-section having an opening is represented in Figure 9, together with regular nodes (•) and additional nodes (×). The opening is not aligned with the Cartesian coordinate system.

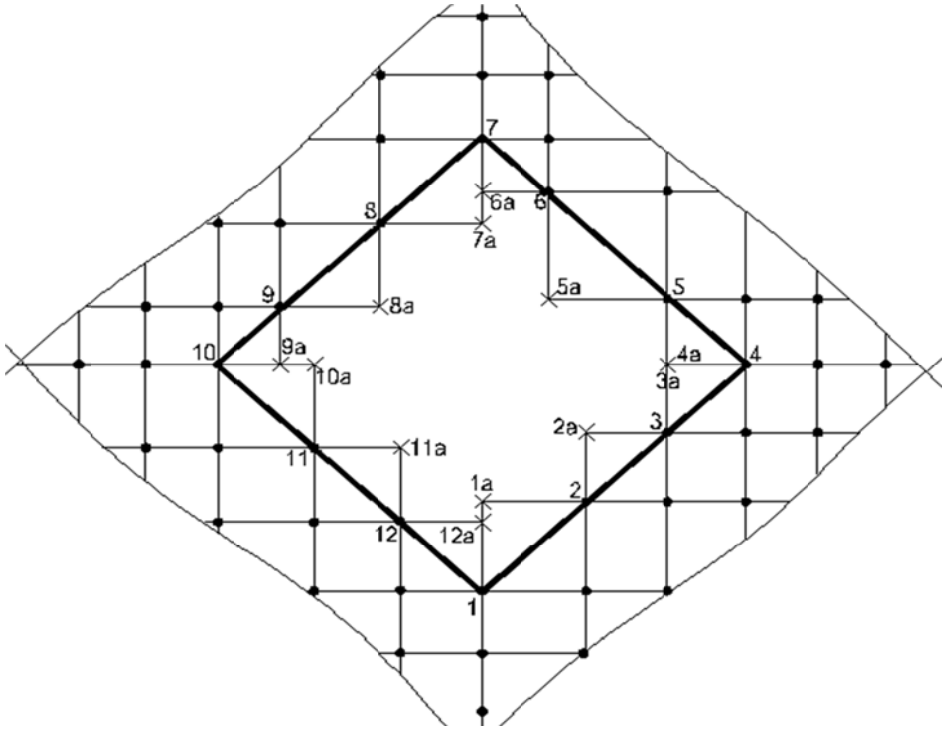


Figure 9 Beam's cross-section having an opening of various shape

It is further assumed that different nodes may be at the same geometrical position, i.e. nodes 4a and 3a. The boundary condition $\psi$ = constant are applied at nodes on the opening; therefore, for Figure 9 eleven boundary conditions are applied. If additional nodes are associated to k nodes on the opening, k + 1 governing equations should be applied in order to have as many nodes as equations; this implies to consider eleven additional nodes in Figure 9 and so to set twelve governing equations. By the formulation of the governing equations and equations determining the shear stresses, especially at angle nodes; those equations at any node k involve the node ka.

Preprints (www.preprints.org) | NOT PEER-REVIEWED | Posted: 31 March 2022 doi:10.20944/preprints202203.0410.v1



## 2.7 Beams with thin-walled sections

### 2.7.1 Fundamentals of thin-walled sections

Given a beam with thin-walled section represented in Figure 10.

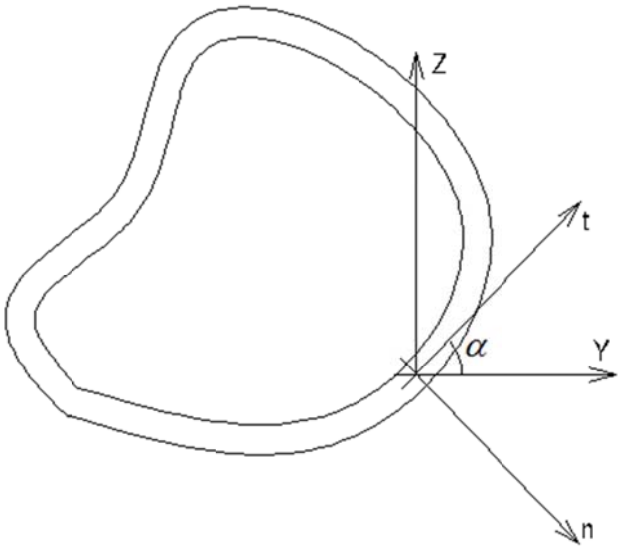


Figure 10 Beam with thin-walled section

At the one hand, the analysis of beams with single-cell thin-walled closed sections i.e. is governed by the following Bredt's formulas for the shear stress $\tau_t$ at an arc coordinate s and the torsion constant It

$$\tau_t(s) = \frac{M_t}{2A_m t(s)}, \qquad I_t = \frac{4A_m^2}{\oint \frac{ds}{t(s)}} \tag{23a-b}$$

where $A_m$ is the area enclosed by the midline of the thin-walled closed section. Bredt's formulas are derived under the assumption of a constant shear stress $\tau_t$ over the thickness whereby stresses $\tau_n$ are neglected.

At the other hand, the analysis of thin-walled open sections is governed by the following formulas

$$\tau_{\max}(s) = \frac{M_t}{I_t} t(s), \qquad I_t = \frac{1}{3}\int t(s)^3 \, ds \tag{23c-d}$$

In the present study, the stress component $\tau_n$ and $\tau_t$ can be defined as follows using a coordinate transformation and observing Figure 2 and Equations (6),

$$\tau_n = \frac{\partial \phi}{\partial t}, \qquad \tau_t = -\frac{\partial \phi}{\partial n} \tag{24a-b}$$

Furthermore, Equations (4), (7), and (13b) are transformed as follows

$$\frac{\partial \tau_n}{\partial t} - \frac{\partial \tau_t}{\partial n} = -2G\frac{d\theta}{dx}, \qquad \frac{\partial^2 \phi}{\partial t^2} + \frac{\partial^2 \phi}{\partial n^2} = -2G\frac{d\theta}{dx}, \qquad \frac{\partial^2 \psi}{\partial t^2} + \frac{\partial^2 \psi}{\partial n^2} = -2 \tag{25a-c}$$

Preprints (www.preprints.org) | NOT PEER-REVIEWED | Posted: 31 March 2022 doi:10.20944/preprints202203.0410.v1



Let us consider continuity regions and discontinuity regions in the cross-section defined as follows: continuity regions that are away from segment ends and angles of the cross-section, are characterized by constant stress function along s while discontinuity regions are segment ends and angles of the cross-section.

### 2.7.2 Thin-walled open sections

At an arc coordinate s the inner and outer node are denoted by si and so, respectively. Recalling that the stress function is constant along the unique boundary, the stress component $\tau_t$ at the midline at position s of thickness t(s) can be determined using Equations (15b) and (24b) as follows

$$\tau_t(s) = -\frac{\partial \phi}{\partial n} = -\frac{\phi_{so} - \phi_{si}}{t(s)} = 0 \tag{26}$$

The stress component $\tau_t$ at the midline is zero: this finding is in agreement with the analysis of thin-walled open sections. Equation (24a) shows that the stress component $\tau_n$ is zero in continuity regions while $\tau_t$ that is zero at midline can be expressed as follows using Equation (25a)

$$\tau_t(s,n) = 2G\frac{d\theta}{dx} \times n \tag{27a}$$

The stress $\tau_t$ can be formulated using the torsion constant It and the torque Mt in Equation (13c) as follows

$$\tau_t(s,n) = 2\frac{M_t}{I_t} \times n \tag{27b}$$

Equation (27b) shows that the stress component $\tau_t$ is linearly distributed over the thickness, zero at midline and maximal at the boundaries as follows

$$\tau_{t,\max}(s) = \pm 2\frac{M_t}{I_t} \times \frac{t(s)}{2} = \pm\frac{M_t}{I_t} \times t(s) \tag{27c}$$

Consequently, the maximal stresses occur at positions with greatest thickness; this finding is in agreement with the analysis of thin-walled open sections. The modified stress function $\psi(s, n)$ defined in Equation (13a) which is zero at $n = \pm t(s)/2$ and satisfies Equation (25c) is given by

$$\psi(s,n) = \frac{t(s)^2}{4}\left(1 - \frac{4n^2}{t(s)^2}\right) \tag{28a}$$

Then, the torsion constant It calculated using Equation (13d) and (28a) is given by

$$I_t = \frac{1}{3}\int t(s)^3 ds \tag{28b}$$

Equation (28b) is a well-known formula in the analysis of thin-walled open sections.

Preprints (www.preprints.org) | NOT PEER-REVIEWED | Posted: 31 March 2022 doi:10.20944/preprints202203.0410.v1



### 2.7.3 Thin-walled closed sections

The analysis of closed thin-walled sections is conducted using the Bredt's formulas (Equations (23a-b)). These formulas are based on the assumptions of constant shear stress $\tau_t$ over the thickness and neglecting the stress component $\tau_n$. First, these assumptions do not satisfy the relationship between the shear stresses (Equation (4)). Second, Bredt's Equation (23a) implies that the total torque is due to the stress component $\tau_t$, and as shown earlier (Equation (12f)), that is inexact. In the following, another approach for the torsional analysis of closed thin-walled sections is presented.

*Single-cell thin-walled section:* The stress function is taken zero along the outer boundary and $\phi_{si}$ along the inner one. The stress component $\tau_t$ at the midline at position s of thickness t(s) can be determined using Equations (15b) and (24b) as follows

$$\tau_t(s) = -\frac{\partial \phi}{\partial n} = -\frac{\phi_{so} - \phi_{si}}{t(s)} = \frac{\phi_{si}}{t(s)} \tag{29}$$

It is worth mentioning that $\phi_{si}$ corresponds to the shear flow of the Bredt's analysis. The stress component $\tau_t$ can also be determined using Equations (9a) as follows

$$\tau_t = \frac{\partial \phi}{\partial z}\cos\alpha - \frac{\partial \phi}{\partial y}\sin\alpha = \frac{\partial \phi}{\partial z}\frac{dy}{ds} - \frac{\partial \phi}{\partial y}\frac{dz}{ds} \rightarrow \tau_t ds = \frac{\partial \phi}{\partial z}dy - \frac{\partial \phi}{\partial y}dz \tag{30}$$

Let us perform a line integral through the midline using Equations (7), (13a), and (29-30) and the Green's theorem

$$\oint_M \tau_t ds = \oint_M \frac{\phi_{si}}{t(s)} ds = \oint_B \left[\frac{\partial \phi}{\partial z}dy - \frac{\partial \phi}{\partial y}dz\right] = \iint_A \left[-\frac{\partial^2 \phi}{\partial y^2} - \frac{\partial^2 \phi}{\partial z^2}\right] dydz = 2G\frac{d\theta}{dx}A_M$$

$$\rightarrow \oint_M \frac{\psi_{si}}{t(s)} ds = 2A_M \rightarrow \psi_{si} = \frac{2A_M}{\oint_M \frac{ds}{t(s)}} \tag{31}$$

where $A_M$ is the area enclosed by the midline of the cross-section. The modified stress function $\psi(s, n)$ defined in Equation (13a) which is zero and $\psi_{si}$ at $n = \pm t(s)/2$, respectively, and satisfies Equation (25c) is given by

$$\psi(s,n) = \psi_{si}\left(\frac{1}{2} - \frac{n}{t(s)}\right) + \frac{t(s)^2}{4}\left(1 - \frac{4n^2}{t(s)^2}\right) \tag{32a}$$

The torsion constant It is calculated using Equations (14b), (31), and (32a) as follows

$$I_t = \frac{2AA_M}{\oint_M \frac{ds}{t(s)}} + \frac{1}{3}\oint_M t(s)^3 ds + \frac{4A_M A_i}{\oint_M \frac{ds}{t(s)}} \tag{32b}$$

Preprints (www.preprints.org) | NOT PEER-REVIEWED | Posted: 31 March 2022 doi:10.20944/preprints202203.0410.v1



where $A_i$ is the area enclosed by the inner boundary of the cross-section and A is the area of the cross-section material. This expression of the torsion constant coincides with that of Bredt (Equation (23b)) for very small thicknesses.

In continuity regions, the stress component $\tau_n$ is zero and $\tau_t$ is as follows using Equations (25a) and (29).

$$\tau_t(s,n) = 2G\frac{d\theta}{dx}\times n + \frac{\phi_{si}}{t(s)} \tag{33a}$$

Equation (33a) shows that at a position s the stress component $\tau_t$ is linearly distributed over the thickness, maximal and minimal at the boundaries. Using Equations (13c) and (31) $\tau_t$ is given by

$$\tau_{t,\max,\min}(s) = \frac{M_t}{I_t}\times\left(\pm t(s) + \frac{1}{t(s)}\times\frac{2A_M}{\oint_M \frac{ds}{t(s)}}\right) \tag{33b}$$

Equation (33b) shows that contrarily to the Bredt's formulas the maximal shear stress does not necessary occur at the position with the smallest thickness.

*Multiple-cell thin-walled section:* The stress function is taken zero along the outer boundary and $\phi_{sk}$ along the inner boundary of a cell k. For a given cell at a position s the stress function at the inner and outer boundary are denoted by $\phi_{si}$ and $\phi_{so}$ , respectively. So, the stress component $\tau_t$ at the midline at position s of thickness t(s) is as follows

$$\tau_t(s) = -\frac{\partial\phi}{\partial n} = -\frac{\phi_{so}-\phi_{si}}{t(s)} = \frac{\phi_{si}-\phi_{so}}{t(s)} \tag{34a}$$

Equation (31) is applied at each cell through the midline using Equations (13a) and (34a); for the cell k it yields

$$\oint_k \frac{\psi_{si}-\psi_{so}}{t(s)}ds = 2A_{Mk} \tag{34b}$$

For a cell k with thickness $t_k(s)$ bordered by q cells with thickness $t_q(s)$ Equation (34b) can be expressed as follows

$$\psi_k\oint_k\frac{ds}{t_k(s)} - \sum_q \psi_q\int\frac{ds}{t_q(s)} = 2A_{Mk} \tag{34c}$$

So, the values $\psi_k$ of the modified stress function at the inner boundaries of the cells can be determined. $\psi(s, n)$ defined in Equation (13a) with values $\psi_{so}$ and $\psi_{si}$ at $n = \pm t(s)/2$, respectively, which satisfies Equation (25c) is given by

$$\psi(s,n) = \psi_{si}\left(\frac{1}{2}-\frac{n}{t(s)}\right) + \psi_{so}\left(\frac{1}{2}+\frac{n}{t(s)}\right) + \frac{t(s)^2}{4}\left(1-\frac{4n^2}{t(s)^2}\right) \tag{35a}$$

Preprints (www.preprints.org) | NOT PEER-REVIEWED | Posted: 31 March 2022 doi:10.20944/preprints202203.0410.v1



The torsion constant It is then calculated using Equation (14b) and (35a) as follows

$$I_t = \int \left(\psi_{si} + \psi_{so}\right) t(s) ds + \frac{1}{3}\int t(s)^3 ds + 2\sum_k \psi_k A_k \tag{35b}$$

As example the analysis of a three-cell thin-walled section is presented in Appendix B whereby the values $\psi_k$ and the torsion constant are calculated.

In continuity regions, the stress component $\tau_n$ is zero and $\tau_t$ is as follows using Equations (25a) and (34a)

$$\tau_t(s,n) = 2G\frac{d\theta}{dx}\times n + \frac{\phi_{si} - \phi_{so}}{t(s)} = \frac{M_t}{I_t}\times\left(2n + \frac{\psi_{si} - \psi_{so}}{t(s)}\right) \tag{36a}$$

Similarly to the single-cell thin-walled section, the stress component $\tau_t$ at a position s is linearly distributed over the thickness, maximal and minimal at the boundaries as follows

$$\tau_{t,\max,\min}(s) = \frac{M_t}{I_t}\times\left(\pm t(s) + \frac{\psi_{si} - \psi_{so}}{t(s)}\right) \tag{36b}$$

## 2.8 Warping of the cross-section

In the following the cross-sections are assumed free to warp. For a given cross-section and torque the values of the stress function $\psi(y,z)$ were determined according to previous sections. Substituting Equations (3a-b) into (5) yields

$$\frac{\partial^2 u}{\partial y^2} + \frac{\partial^2 u}{\partial z^2} = 0 \tag{37a}$$

Substituting Equations (13a) and (13c) into (3a-b) yields

$$\frac{GI_t}{M_t}\frac{\partial u}{\partial y} = z - z_T + \frac{\partial \psi}{\partial z}, \qquad \frac{GI_t}{M_t}\frac{\partial u}{\partial z} = -y + y_T - \frac{\partial \psi}{\partial y} \tag{37b}$$

Equation (37a) is the governing equation applied at any node of the cross-section, and Equations (37b) are set as boundary conditions. For convenience the node distribution is taken the same as that for the stress function. So, the governing equation (Equation (37a)) is expressed similar to that of the stress function (Equations (16) and (19)); however, zero is put in place of the right-hand side of the latter equations. A modified warping U is defined as U = GIt/Mt × u; therefore, Equations (37a) and (37b) become

$$\frac{\partial^2 U}{\partial y^2} + \frac{\partial^2 U}{\partial z^2} = 0$$
$$\frac{\partial U}{\partial y} = z - z_T + \frac{\partial \psi}{\partial z}, \qquad \frac{\partial U}{\partial z} = -y + y_T - \frac{\partial \psi}{\partial y} \tag{38a-c}$$

Preprints (www.preprints.org) | NOT PEER-REVIEWED | Posted: 31 March 2022 doi:10.20944/preprints202203.0410.v1



In Equations (38b-c) the derivatives of U and ψ are expressed using the stencils in Equations (17) and (20a-b).

A kinematic boundary condition is needed for solving the warping problem. Therefore, at the center of torsion $T\ (y_T, z_T)$ (equivalent to the shear center) the warping is set to zero and the governing equation is not applied.

# 3 Results and discussions

## 3.1 Torsion of beam with rectangular cross-section

The elastic torsional behavior of a beam with rectangular cross-section was analyzed. The dimensions of the cross-section in y- and z-directions are denoted by a and b, respectively. The torsion constant $It = k_1 ba^3$ and the maximal shear stress $\tau_{max} = ka\ Gd\theta/dx$ are determined, depending on the ratio b/a. A 4 × 4, 8 × 8, and 12 × 12 element mesh are considered. Details of the analysis and results are presented in Appendix A and in the supplementary material "Torsion of beam with rectangular cross-section." Table 1 lists the results obtained with Timoshenko [13] using the membrane analogy (exact results) and those obtained in the present study.

Table 1 Coefficients of the torsion constant and maximal shear stress

| | **b/a =** | | | | | | | | | |
|---|---|---|---|---|---|---|---|---|---|---|
| | **1.00** | | **1.50** | | **2.00** | | **3.00** | | **10.00** | |
| | **$k_1$** | **k** | **$k_1$** | **k** | **$k_1$** | **k** | **$k_1$** | **k** | **$k_1$** | **k** |
| | **Solution by Timoshenko [13] (exact results)** | | | | | | | | | |
| | 0.141 | 0.675 | 0.196 | 0.848 | 0.229 | 0.930 | 0.263 | 0.985 | 0.312 | 1.000 |
| | **Present study (Finite Difference Method)** | | | | | | | | | |
| **4 × 4 elements** | 0.133 | 0.688 | 0.185 | 0.838 | 0.215 | 0.913 | 0.243 | 0.971 | 0.270 | 1.000 |
| **8 × 8 elements** | 0.140 | 0.677 | 0.194 | 0.844 | 0.227 | 0.925 | 0.260 | 0.982 | 0.298 | 1.000 |
| **12 × 12 elements** | 0.140 | 0.676 | 0.195 | 0.846 | 0.228 | 0.928 | 0.262 | 0.984 | 0.305 | 1.000 |

As Table 1 shows, the results using FDM show good agreement with the exact results, and the accuracy is increased through a grid refinement. For high values of b/a, the torsion constant It is equal to $1/3 \times ba^3$.

The warping is calculated for a beam with dimensions a = b = 1.0m for a unity torque, whereby a 12 × 12 mesh is considered. Recalling that the stress function ψ = 0 along the boundary, the boundary conditions are set observing that ∂ψ/∂z is zero along the edges y = ± a/2 and ∂ψ/∂y is zero along the edges z = ± b/2. Details of the results are presented in the above mentioned supplementary material. The factored warping $G \times u = U/It$ is given in Table 2.

Preprints (www.preprints.org) | NOT PEER-REVIEWED | Posted: 31 March 2022 doi:10.20944/preprints202203.0410.v1



Table 2 Factored warping G × u for a beam with dimensions a = b = 1.0m and Mt = 1.0 MNm

| | | | | | | | | | | | | |
|---|---|---|---|---|---|---|---|---|---|---|---|---|
| -0.151 | 0.104 | 0.202 | 0.212 | 0.168 | 0.091 | 0.000 | -0.091 | -0.168 | -0.212 | -0.202 | -0.104 | 0.151 |
| -0.270 | -0.064 | 0.048 | 0.090 | 0.085 | 0.049 | 0.000 | -0.049 | -0.085 | -0.090 | -0.048 | 0.064 | 0.270 |
| -0.306 | -0.139 | -0.035 | 0.017 | 0.031 | 0.022 | 0.000 | -0.022 | -0.031 | -0.017 | 0.035 | 0.139 | 0.306 |
| -0.279 | -0.152 | -0.068 | -0.019 | 0.003 | 0.006 | 0.000 | -0.006 | -0.003 | 0.019 | 0.068 | 0.152 | 0.279 |
| -0.208 | -0.123 | -0.064 | -0.027 | -0.008 | -0.001 | 0.000 | 0.001 | 0.008 | 0.027 | 0.064 | 0.123 | 0.208 |
| -0.111 | -0.068 | -0.037 | -0.018 | -0.007 | -0.002 | 0.000 | 0.002 | 0.007 | 0.018 | 0.037 | 0.068 | 0.111 |
| 0.000 | 0.000 | 0.000 | 0.000 | 0.000 | 0.000 | 0.000 | 0.000 | 0.000 | 0.000 | 0.000 | 0.000 | 0.000 |
| 0.111 | 0.068 | 0.037 | 0.018 | 0.007 | 0.002 | 0.000 | -0.002 | -0.007 | -0.018 | -0.037 | -0.068 | -0.111 |
| 0.208 | 0.123 | 0.064 | 0.027 | 0.008 | 0.001 | 0.000 | -0.001 | -0.008 | -0.027 | -0.064 | -0.123 | -0.208 |
| 0.279 | 0.152 | 0.068 | 0.019 | -0.003 | -0.006 | 0.000 | 0.006 | 0.003 | -0.019 | -0.068 | -0.152 | -0.279 |
| 0.306 | 0.139 | 0.035 | -0.017 | -0.031 | -0.022 | 0.000 | 0.022 | 0.031 | 0.017 | -0.035 | -0.139 | -0.306 |
| 0.270 | 0.064 | -0.048 | -0.090 | -0.085 | -0.049 | 0.000 | 0.049 | 0.085 | 0.090 | 0.048 | -0.064 | -0.270 |
| 0.151 | -0.104 | -0.202 | -0.212 | -0.168 | -0.091 | 0.000 | 0.091 | 0.168 | 0.212 | 0.202 | 0.104 | -0.151 |

.

The distortions are zero in the symmetry axes of the beam and greatest in the sides between the axis and the angles.

### 3.2 Torsion of beam with thin-walled sections

The elastic torsional behavior of a beam with closed thin-walled sections, as represented in Figure 11, was analyzed. The dimensions of the cross-section in y- and z-directions are denoted by a = 1.0m and b = 1.0m, respectively. The thickness t is chosen a/6, a/8, a/10, a/15, and a/20.

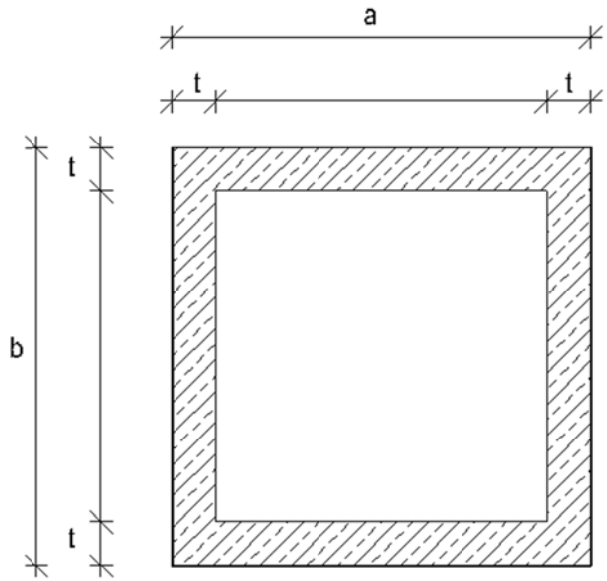


Figure 11 Beam with rectangular thin-walled section

Preprints (www.preprints.org) | NOT PEER-REVIEWED | Posted: 31 March 2022 doi:10.20944/preprints202203.0410.v1



The shear stresses $\tau_t$ are determined for a torque Mt = 1.0 kNm for numerous values of thicknesses. Details of the results are presented in the supplementary material "Torsion of beam with thin-walled sections." The results obtained in the present study are compared to those using Bredt's formulas (Equations (23a-b)) and are listed in Table 3.

Table 3 Shear stresses and torsion constant for the thin-walled closed section

| | | t = a/6 | a/8 | a/10 | a/15 | a/20 |
|---|---|---|---|---|---|---|
| **Shear stress $\tau_t$ Bredt** | | 4.32 | 5.22 | 6.17 | 8.61 | 11.08 |
| **Shear stresses $\tau_t$** | **Outer boundary** | 5.53 | 6.41 | 7.33 | 9.72 | 12.17 |
| | **Midline** | 3.95 | 4.99 | 6.00 | 8.51 | 11.01 |
| | **Inner boundary** | 2.37 | 3.56 | 4.67 | 7.29 | 9.85 |
| **Torsion Constant It ( Bredt )** | | 0.0965 | 0.0837 | 0.0729 | 0.0542 | 0.0429 |
| **Torsion Constant It (Present study)** | | 0.1055 | 0.0877 | 0.0750 | 0.0548 | 0.0431 |

The shear stresses in this study vary linearly over the thickness. As Table 3 shows, this paper presents values of shear stresses at midline close to those of Bredt but the maximal values are higher. It is noted that for very small values of thickness, the results converge towards those of Bredt.

## 4 Conclusion

The FDM-based model developed in this paper enables, with certain easiness, the elastic analysis of beams subjected to Saint-Venant torsion. The results showed that the calculations, as described in this paper, yield accurate results. Beams with thin-walled sections were also analyzed and closed form solutions were presented; these solutions accounting for the linear distribution of the shear stresses over the thickness can be regarded as an improvement of the Bredt's analysis.

The following aspect was not addressed in this study but could be analyzed with the model in future research:

✓ Analysis of beams with thin-walled sections using FDM

**Supplementary Materials:** The following files were uploaded during submission:

- "Torsion of beam with rectangular cross-section"
- "Torsion of beam with thin-walled sections."

Preprints (www.preprints.org) | NOT PEER-REVIEWED | Posted: 31 March 2022 doi:10.20944/preprints202203.0410.v1

# Cross-sectional Analysis of Beams Subjected to Saint-Venant Torsion

**Funding:**

**Acknowledgments:**

**Conflicts of Interest:** The author declares no conflict of interest.

## Appendix A Beam with rectangular cross-section

Given a beam with rectangular cross-section and known values of $\psi$. The integral $\int\psi dydz$ needed for the torsion constant It is determined here. The grid spacings in y- and z-direction are denoted by $\Delta y$ and $\Delta z$, respectively. The cross-section is divided in rectangles around grid points, as represented in Figure 12.

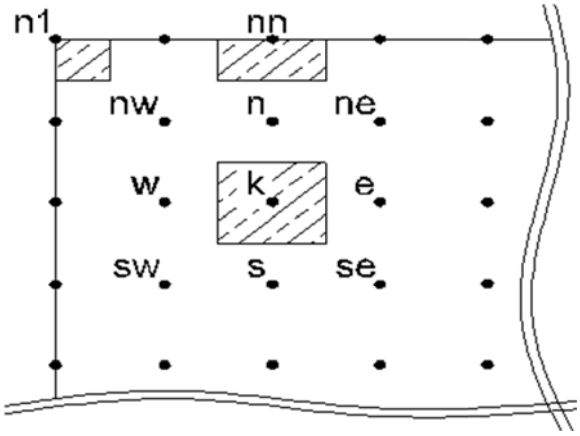


Figure 12 Rectangles for the calculation of the torsion constant

Given the rectangle bounded by nodes k, e, s, and se in Figure 12. The stress function $\psi(y,z)$ is approximated as follows

$$\psi(y,z) = \psi_k f_k(y,z) + \psi_e f_e(y,z) + \psi_s f_s(y,z) + \psi_{se} f_{se}(y,z) \quad \text{(A1)}$$

The shape function $f_e(y,z)$ i.e. can be expressed as follows

$$f_e(y,z) = \frac{yz}{\Delta y \times \Delta z} \quad \text{(A2)}$$

Using Equations (A1) and (A2), the integral for the rectangle of interest is

$$\iint \psi dydz = \frac{1}{4}\left(\psi_k + \psi_e + \psi_s + \psi_{se}\right) \times \Delta y \times \Delta z \quad \text{(A3)}$$

Using Equation (A3) for a uniform grid, $\int\psi dydz$ on a rectangle around an interior node (node k) is $\psi_k \Delta y \Delta z$. Similarly, using Equation (A3) and recalling that the values of $\psi$ are zero along the boundary, the integral for a rectangle around a boundary node (node nn) is $1/8 \times \psi_n \Delta y \Delta z$, and for a rectangle around an angle node (node n1) $1/64 \times \psi_{nw} \Delta y \Delta z$.

Preprints (www.preprints.org) | NOT PEER-REVIEWED | Posted: 31 March 2022 doi:10.20944/preprints202203.0410.v1



## Appendix B Three-cell thin-walled section

The values $\psi_k$ of the modified stress function at the inner boundaries of the cells are determined for the three-cell thin-walled section represented in Figure 13.

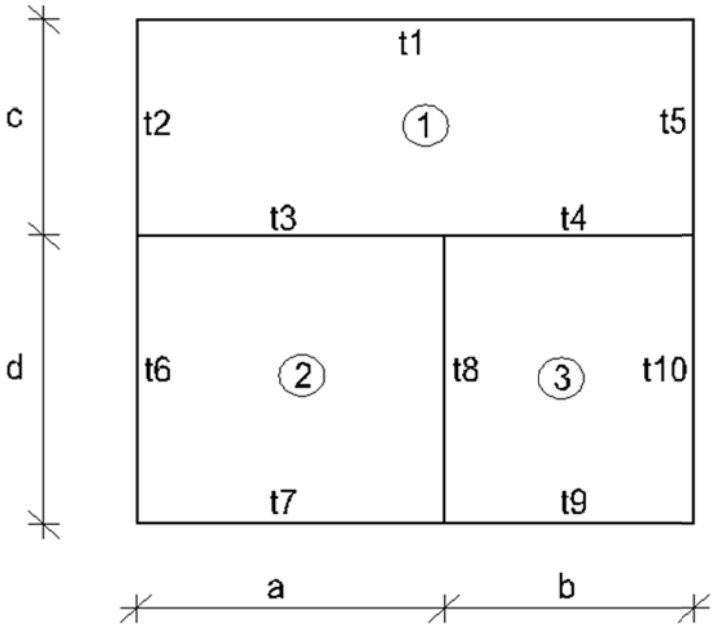


Figure 13 Three-cell thin-walled section

Let $\psi_1$, $\psi_2$, and $\psi_3$ be the values of the modified stress function at the inner boundaries of the cells 1, 2, and 3, respectively; they are solutions of the following system of equations using Equation (34**c**) applied at each cell

$$\begin{aligned}
&\psi_1\left[\frac{a+b}{t_1}+\frac{c}{t_2}+\frac{a}{t_3}+\frac{b}{t_4}+\frac{c}{t_5}\right]-\psi_2\frac{a}{t_3}-\psi_3\frac{b}{t_4}=2A_{M1}\\
&\psi_2\left[\frac{a}{t_3}+\frac{d}{t_6}+\frac{a}{t_7}+\frac{d}{t_8}\right]-\psi_1\frac{a}{t_3}-\psi_3\frac{d}{t_8}=2A_{M2}\\
&\psi_3\left[\frac{b}{t_4}+\frac{d}{t_8}+\frac{b}{t_9}+\frac{d}{t_{10}}\right]-\psi_1\frac{b}{t_4}-\psi_2\frac{d}{t_8}=2A_{M3}
\end{aligned} \tag{B1}$$

where $A_{Mi}$ are the areas enclosed by the midline of the cell i. The torsion constant is determined using Equation (35b) recalled below

$$I_t=\int\left(\psi_{si}+\psi_{so}\right)t(s)ds+\frac{1}{3}\int t(s)^3ds+2\sum_k\psi_kA_k \tag{B2}$$

Preprints (www.preprints.org) | NOT PEER-REVIEWED | Posted: 31 March 2022 doi:10.20944/preprints202203.0410.v1



where $A_i$ are the areas enclosed by the inner boundary of the cell i. The first term at the right-hand side of Equation (B2) is calculated as follows

$$\begin{aligned}\int \left(\psi_{si}+\psi_{so}\right)t(s)ds = {} & \psi_1\left(a+b\right)t_1+\psi_1 ct_2+\left(\psi_1+\psi_2\right)at_3 \\ & +\left(\psi_1+\psi_3\right)bt_4+\psi_1 ct_5+\psi_2 dt_6+\psi_2 at_7 \\ & +\left(\psi_2+\psi_3\right)dt_8+\psi_3 bt_9+\psi_3 dt_{10}\end{aligned} \tag{B3}$$

## References


[1] Fogang, V. Euler-Bernoulli Beam Theory: First-Order Analysis, Second-Order Analysis, Stability, and Vibration Analysis Using the Finite Difference Method. Preprints 2021, 2021020559 (doi: 10.20944/preprints202102.0559.v3).

[2] Saint-Venant, B. Mémoires savants étrangers, vol. 14, 1855

[3] Prandtl, L. Physik. Z., vol. 4, 1903.

[4] Ritz, W. J. reine angew. Math., vol. 135, 1908

[5] Trefftz, E. Proc. Second Intern. Congr. Applied Mech., Zürich, 1926, p.131

[6] Pluzsik, A., Kollar, L.P. Torsion of closed section, orthotropic, thin-walled beams. IJSS, Volume 43, Issue 17, August 2006, Pages 5307-5336. https://doi.org/10.1016/j.ijsolstr.2005.08.001

[7] Pan, W.-H., Zhao, C.-H., Tian, Y., Lin, K.-Q. Exact Solutions for Torsion and Warping of Axial-Loaded Beam-Columns Based on Matrix Stiffness Method. Nanomaterials 2022, 12, 538. https://doi.org/10.3390/nano12030538

[8] Pavazza, R., Matoković, A., Vukasović M. 2022. A theory of torsion of thin-walled beams of arbitrary open sections with influence of shear, Mechanics Based Design of Structures and Machines, 50:1, 206-241, DOI: 10.1080/15397734.2020.1714449

[9] Choi, S., Kim, Y. Y. Higher-order Vlasov torsion theory for thin-walled box beams. IJMS, Volume 195, 1 April 2021, 106231. https://doi.org/10.1016/j.ijmecsci.2020.106231

[10] Amulu, C. P., Ezeagu, C. A. Experimental and Analytical Comparison of Torsion, Bending Moment and Shear Forces in Reinforced Concrete Beams Using BS 8110, Euro Code 2 and ACI 318 Provisions. NIJOTECH, Vol. 36, No. 3, July 2017, pp. 705 – 711. http://dx.doi.org/10.4314/njt.v36i3.7

[11] Tran, D.-B. (2021). Torsional Shear Stress in Prismatic Beams With Arbitrary Cross-Sections Using Finite Element Method. *Stavební Obzor - Civil Engineering Journal*, *30*(2). https://doi.org/10.14311/CEJ.2021.02.0030

[12] Dieker, S., Reimerdes, H-G. Elementare Festigkeitslehre im Leichtbau. Donat Verlag, Bremen. 1992. ISBN 3-924444-58-7

[13] Timoshenko, S., Goodier, J. N. Theory of elasticity. McGraw-Hill Book Company, Inc., New York, 2nd edition, 1951